**Proceedings of the 27th Annual Fellowship Symposium**
**of the Utah NASA Space Grant Consortium**
**UNSGC 2021**
**May 10, 2021, Logan, UT, USA**

# ASSESSING THICKNESS ACCOMMODATION TECHNIQUES FOR DEPLOYABLE HEXAGONAL ORIGAMI SPACE ARRAYS

**Collin Ynchausti***
Compliant Mechanism Research
Department of Mechanical Engineering
Brigham Young University
Provo, UT 84602
Email: collinynchausti@byu.net

**Larry L. Howell**
Compliant Mechanism Research
Department of Mechanical Engineering
Brigham Young University
Provo, UT 84602
lhowell@byu.edu

## ABSTRACT

*Origami-based and origami-inspired designs provide paths to achieve highly compact, stowable designs, that can be deployed to large surface areas. This potential is highly beneficial to the area of space antennas and LIDAR as these require compact stowing in a launch payload, but large apertures when deployed in space. Because the engineering materials used to build these antennas are thick, thickness accommodation techniques must be applied to realize the same folding motions as the zero-thickness models. This paper presents a hexagonal twist origami pattern in thick materials using three different thickness accommodation techniques. These techniques are compared. The metrics used for comparison are packing efficiency, usable area, benefit to stability, and deployment methods. These metrics have also help to determine trends that can benefit the designer when selecting thickness accommodation techniques.*

## 1 INTRODUCTION

Due to the increasing use of collaborative, ride-along efforts being carried out in the space-exploration field currently [1–4], solutions that utilize this effort need to be readily stowable, utilizing stowed space effectively and efficiently. Additionally, for power and communication applications, large apertures are required as the size of the aperture directly relates to the efficiency of the system [5]. Deployable systems address both of the above needs; they can be stowed compactly, then deployed to much larger areas or volumes at the desired operating location.

The specific requirements for reflectarray antennas and light detection and ranging (LIDAR) telescopes are used here as these are the presented design cases. For reflectarray antennas, the larger the aperture the better [5]. The required flatness of these types of antennas is between $\frac{1}{20}th$ to $\frac{1}{40}th$ of the wavelength that they are designed to receive [6, 7]. For LIDAR telescopes, many of the requirements are the same. The larger the aperture, the more power that can be received [8]. With both reflectarry and LIDAR telescopes, it is beneficial to have the surface of the aperture be on the same plane. However, flat, parallel surfaces can be used, with added design work required.

Deployable systems have been used throughout space-exploration efforts as the main focus for design, in these cases, is the size of the system, the weight of the system, and the power the system can generate (SWaP) [9]. However, many of these deployable systems use associated deployment systems, such as booms or trusses to assist in the deployment. These systems require more volume in the launch vehicle payload. Origami has inspired deployable designs that have allowed researchers and designers to realize large area gain from a stowed to compact shape. However, even origami proves challenging when attempting to deploy and stop the pattern in a completely flat position.

Additionally, most origami fold patterns are developed using zero-thickness models. Most engineering materials are not zero-thickness, requiring different techniques to account for this thickness while still allowing the origami-inspired mechanisms

*Address all correspondence to this author.

to fold as desired.

## 2 BACKGROUND

Origami is the ancient art of paper folding. This art has recently inspired researchers in solving many different design problems. Areas where origami has been implemented include the actuation of systems [10], as a mechanism in supporting catheters [11] and other biomedical applications [12], space applications [13–15], and consumer products [16]. Different origami patterns were used as inspiration in each case. Yu et al. [10] used the Miura-ori pattern as an actuator. Sargent et al. [11] used the Kresling pattern to tune the mechanism to have a certain desired bistability. Al-Mansoori et al. [17] showed ways to manufacture the Kresling and a flasher pattern in carbon fiber composites. Wang et al. [18] used a square-twist origami pattern to create a reconfigurable antenna. De Figueiredo et al. [16] used the square twist, chicken wire, and a modified hexagonal twist patterns to present objects during actuation of conceal and reveal boxes. Many different patterns have proved beneficial for different design cases. The work presented here is based on the hexagonal twist pattern as presented by Tolman [19].

### 2.1 Hexagonal Twist Pattern

The hexagonal twist pattern is flat-foldable, meaning it will fold flat without panel interference in the open and closed configurations. The pattern is also rigid-foldable. This pattern was shown in [19] and is reproduced in Fig. 1.(a) for the benefit of the reader. Figure 1.(b), (c), and (d) show the fold progression from the open configuration to the flat, closed configuration. Figure 1.(a) also shows that the pattern is an array of repeating degree-4 vertices. The sector angles of these vertices are $\alpha_1 = 90^o$, $\alpha_2 = 60^o$, $\alpha_3 = 90^o$, and $\alpha_4 = 120^o$.

### 2.2 Rigid-Foldable Origami

Because the hexagonal twist pattern is rigid-foldable and portions of the design depend on these relations, a short discussion on rigid-foldability will be presented. Rigid-foldable patterns allow the desired folding of the pattern through the deformation of the creases only. Because no deformation occurs in the panels during folding, relations can be made between the sector angles of the pattern and the fold angles. Figure 2 shows a symmetric degree-4 vertex. For any generic, flat-foldable degree-4 vertex there are relations between the sector angles and the fold angles. These relationships, presented by Lang [20] and others, are

$$\begin{aligned} \gamma_1 &= -\gamma_3 \\ \gamma_2 &= \gamma_4 \end{aligned} \tag{1}$$

$$\frac{\tan(\frac{1}{2}\gamma_2)}{\tan(\frac{1}{2}\gamma_1)} = \frac{\sin(\frac{1}{2}(\alpha_1+\alpha_2))}{\sin(\frac{1}{2}(\alpha_1-\alpha_2))} \tag{2}$$

where $\gamma_i$ is the fold angle between the $(i-1)$ and $i^{th}$ panels and $\alpha_i$ represents the sector angle of the $i^{th}$ panel, which is the angle between the creases of that panel. Specifying the sector angles, $\alpha$, one fold angle, $\gamma$, and using these relationships, the complete folding motion of the degree-4 vertex can be determined.

The model shown in Fig. 1 is the zero-thickness pattern. Because most material used in engineered products has some thickness, different techniques must be used to design for these thicknesses, while allowing the pattern to still move.

### 2.3 Thickness Accommodation Techniques

One of the earliest techniques for thickness accommodation was proposed by Tachi [21]. This technique is known as "Tapered Panels" technique. Material is removed from the edges of each thickened panel, creating a taper on each panel, to allow the thick array to fold. However, this technique eliminates the possibility of the pattern folding fully flat. Edmondson et al. [22] proposed the offset panel technique. This technique keeps the hinges on the zero-thickness model and allows the array to fold flat, however, it moves the panels away from this axis with attachments to these hinges. Depending on the panel thickness, this technique may require much more thickness in the out-of-plane direction. Lang et al. [23] presented a technique that using rolling joints with shapes that synchronize the motion of panels moving at different relative rotational velocities. The joints are termed synchronized offset rolling contact elements (SORCE) joints. Other techniques have been presented and are reviewed by Lang et al. [24]. In this present work, the three techniques above will be evaluated as applied to the hexagonal twist pattern.

## 3 MODIFIED HEXAGONAL TWIST

Because an increase in the deployed area of an origami pattern will increase the gain of the a reflectarray antenna or a LIDAR telescope, the hexagonal twist shown in Fig. 1.(a) was modified to increase the deployed area, without affecting any other panels during the folding motion or in the flat, closed configuration. Figure 3.(b) shows the modified hexagonal twist. In Fig. 3.(a), the triangular panels of the original pattern fold, however, they do not completely cover the pentagonal pattern.

To maximize the deployed area, the panel shape could be changed as long as it does not interfere with the folding or the stowing of the overall pattern. Figure 3.(b) shows the largest shape that can be placed within this pattern without panel interference. This shape is a rhombus. This change is shown with

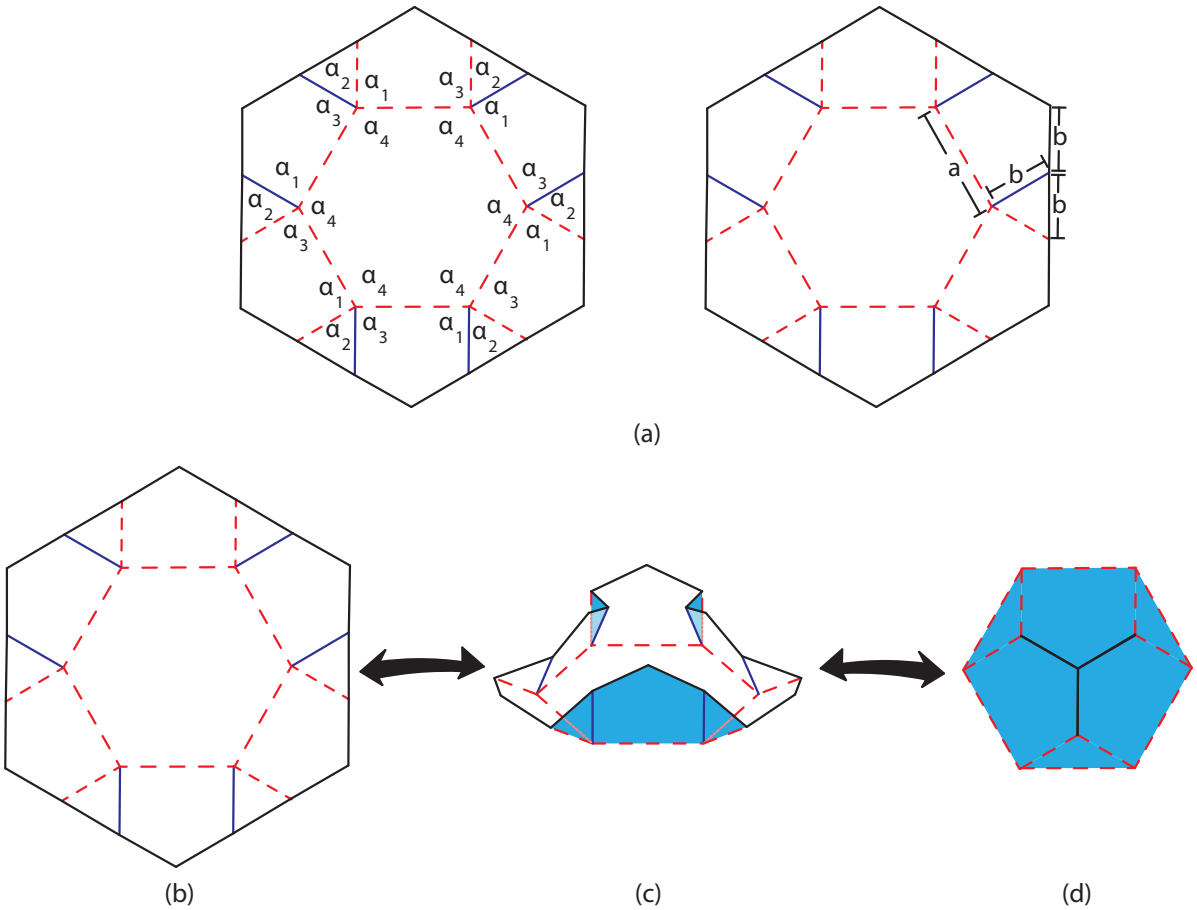


**FIGURE 1**: (a) The hexagonal twist fold pattern. Mountain folds are shown as solid, blue lines. Valley folds are shown as dashed, red lines. The sector angles of all degree-4 vertices in the pattern are also shown. The second pattern shows the lengths of different portions of the pattern. (b) The hexagonal twist in the flat, open configuration. (c) The pattern partially folded. The white panels represent the top of the pattern as shown in (b). Blue panels represent the backside of the panels and pattern. Hidden lines are shown with an increased dash. Hidden panels are shown in a lighter blue color. (d) The hexagonal twist fold pattern in the flat, closed configuration.

the offset panel technique presented later in this paper. As a note, figures of the other techniques do not show this change, however, all calculations presented in this paper consider this change from a triangular to a rhombus panel. Values of the hexagonal parameters as shown in Fig. 1.(a) are presented in Table 1.

## 4 METRICS FOR COMPARISON OF TECHNIQUES

Metrics used to compare thickness accommodation techniques have been determined based on SWaP requirements, requirements specific to reflectarrays and LIDAR telescopes, and requirements regarding deployment.

### 4.1 Packing Efficiency

Packing efficiency is an important metric because it determines how well the volume that the pattern is being placed into is being used. In order to determine the packing efficiency, the following equation is used.

$$\eta_{packing} = \frac{V_p}{V_{sc}} \tag{3}$$

where $\eta_{packing}$ is the packing efficiency, $V_p$ is the volume of the pattern, and $V_{sc}$ is the volume of the smallest cuboid that the stowed pattern fits into. A value of 1 is the maximum value of the packing efficiency because this represents a pattern that com-

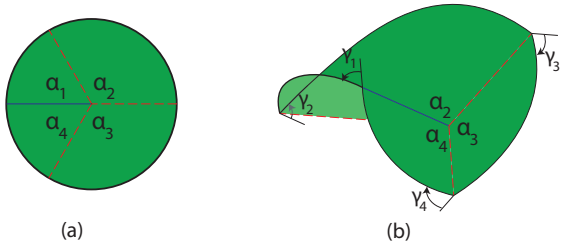


**FIGURE 2**: (a) A degree-4 vertex. The $\alpha_i$ is the sector angle of the $i^{th}$ panel. (b) A degree-4 vertex in the middle of its folding motion. The fold angle between the $i-1$ and $i$ panel is $\gamma_i$.

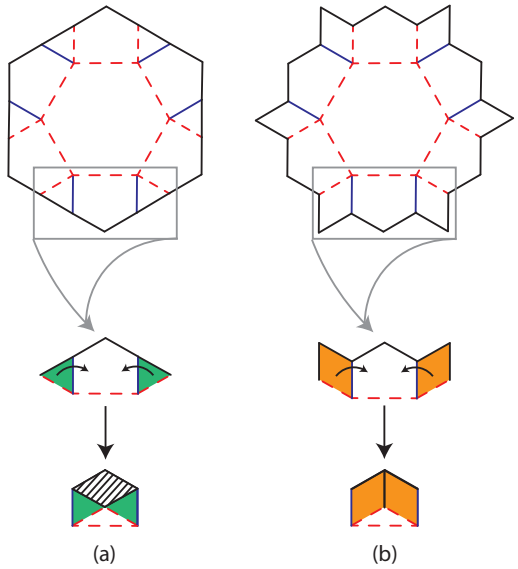


**FIGURE 3**: (a) The hexagonal twist pattern. The area of the pentagonal panel that the triangle panel (green) occupies when folded. The dashed area shows the portion of the panel area that could be covered without interfering with other panels during folding. (b) The modified hexagonal twist pattern. This pattern takes advantage of unused area in the original pattern. The area of the pentagonal panel that the rhombus (orange) occupies when folded. The rhombus occupies the maximum amount of area when folded without interfering with other folded panels.

pletely fills the smallest cuboid. Fig. 4 shows this bounding box for an example hexagonal twist.

### 4.2 Usable Deployed Area

Because power is dependent upon the area of the pattern, the deployed area of each thickness accommodation technique is

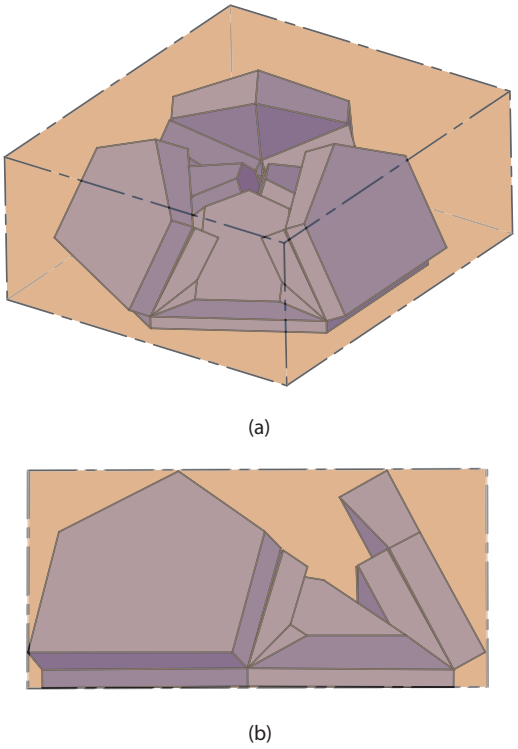


**FIGURE 4**: (a) The smallest rectangular cuboid that fits around the stowed tapered-panel hexagonal twist from an isometric view. (b) A side view of the thickened pattern and cuboid to show the size of the cuboid.

an important metric. The zero-thickness pattern models, that are initially used, assume the the creases are also infinitesimally thin. However, when thick materials are used, area and volume in the pattern are required for hinges.

For the analysis provided here, the projected usable area will be analyzed as this seems the best measure of the deployed

**TABLE 1**: Parameters of the Modified Hexagonal Array.

| Parameter | Value | Units |
|---|---|---|
| Hexagon Side Length (a) | 577.4 | mm |
| Pentagon Length (b) | 333.3 | mm |
| Panel Thickness (t) | 76.2 | mm |

area. The projected usable area is defined as the total area of the hexagon pattern when it is open, projected, onto a parallel plane minus the area that the hinges will take up. The area the hinges require is subtracted from the projected area because the hinges will not allow for either the reflectarray or LIDAR components to be placed there. This leads to usable area ratio ($r_{ua}$) of

$$r_{ua} = \frac{A_{thick}}{A_{total}} = 1 - \frac{A_{hinges}}{A_{total}} \tag{4}$$

where $A_{thick}$ is the usable area of each thickened pattern ($A_{total} - A_{hinges}$) and $A_{total}$ is the total area of the hexagonal pattern.

### 4.3 Deployment

Deployment as discussed here will cover grounding the pattern as well as actuation of the pattern.

**4.3.1 Grounding** First, grounding of the pattern refers to how and where the pattern is attached to the overall system, in this case, a cubesat. In general, the pattern could be grounded at a panel, an edge, or a vertex. As grounding a panel will provide the most contact between the supporting structure and the pattern, only grounding to panels will be discussed.

**4.3.2 Actuation** The three thickness accommodation techniques provide different options for actuation. If a technique allows for more potential actuation types, this technique may help to produce a more versatile design.

Prior origami mechanisms have been actuated using tension-based cabling and use of stored strain energy [25–27]. Both of these ideas could be used in combination or by themselves. Another potential actuation method would be to actuate the pattern at one of the top folded panels. As there is only rotation around crease patterns, a motor could be attached to actuate the pattern.

## 5 THICKNESS ACCOMMODATED HEXAGONAL TWIST

Because both reflectarrays and LIDAR telescopes require using materials that have a thickness, different techniques were applied to the hexagonal twist so that it could be realized in thick materials. The following subsections briefly discuss how each thickness accommodation technique was applied to the hexagonal twist pattern.

### 5.1 OFFSET PANEL HEXAGONAL ARRAY

As discussed above, the offset panel thickness accommodation technique keeps the hinges of the pattern on the zero-thickness model, while moving the panels away from this axis so that the panels can stack together when folded. This technique allows for any thickness of material, however, with greater thicknesses, the panels are moved farther from the zero-thickness axis.

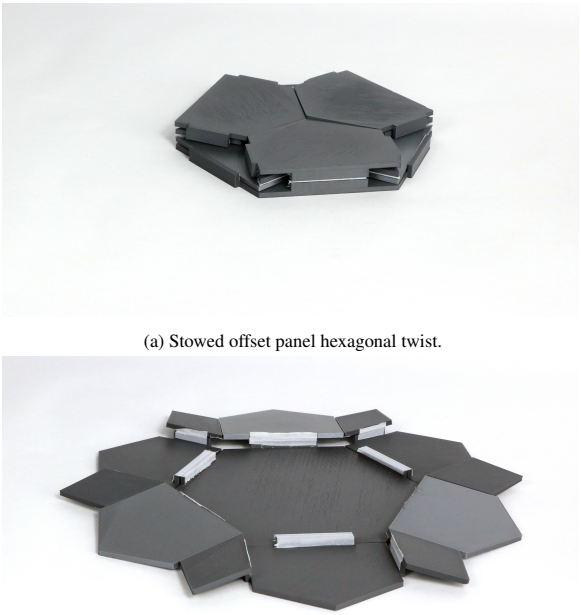

(a) Stowed offset panel hexagonal twist.

(b) Deployed, open configuration of the offset panel hexagonal twist.

**FIGURE 5**: The stowed and deployed states of the offset panel hexagonal twist.

Figure 5 shows the modified hexagonal twist pattern in the offset panel technique. This particular pattern was developed for use as a deployable reflectarray on a cubesat. This array was designed for the panels to be 3 mm thick and accommodate for a 0.8 mm thick Rogers copper-plated ceramic laminate, to be used to receive/transmit the radio frequency (RF) signals.

### 5.2 TAPERED PANEL HEXAGONAL ARRAY

The tapered panel technique was also applied to the hexagonal twist pattern. In order to determine how to correctly taper the panels, the fold angles of each panel are needed to be determined. Because the array will not fold flat using the tapered panel technique, the maximum fold angle that is desired needs to be determined using Eqns. (1) and (2). In the case of the pattern shown in Fig. 6, a fold angle, $\gamma_1$, was determined to be $120^o$. Selecting this value and using the relations of rigid-foldable origami allows the other fold angles to be determined and thus the taper angles can be determined, as it is half of difference of 180 and the fold angles ($\frac{1}{2}(180^o - \gamma_i)$. The thickness of the pattern shown in Fig. 6 is approximately 19 mm. As this maximum fold angle is increased (moves closer to $180^o$), more of the panels are

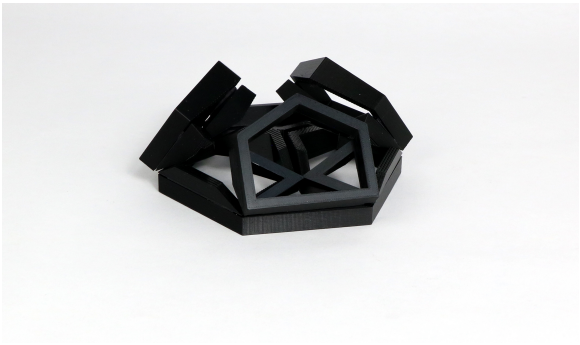

(a) Stowed tapered panel hexagonal twist.

(b) Deployed, open configuration of the tapered panel hexagonal twist.

**FIGURE 6**: The stowed and deployed states of the tapered panel hexagonal twist.

cut away. This removes material that can be used to create hard stops and increase the stability of the pattern.

The holes in each panel of the patterns in Fig. 6 and 7 were created because these arrays were designed and investigated as potential solutions for a LIDAR telescope, requiring areas for light to be focused through.

### 5.3 SYNCHRONIZED OFFSET ROLLING CONTACT ELEMENT (SORCE) HEXAGONAL ARRAY

The SORCE joints were determined using the equations provided in [23]. The determination of the paths of the joints is dependent upon the desired panel thickness. In the case shown in Fig. 7, the initially thickness desired was 76.2 mm. The SORCE joints were determined for this thickness and the pattern was scaled to 15% of the initial size. This yields a thickness of the prototype in Fig. 7 of approximately 11.4 mm.

Figure 7 shows the closed and open positions of the array. Figure 7.(a) shows that the array folds flat using this technique. This technique also provides for all the tops of the panels to be on the same plane when it is deployed.

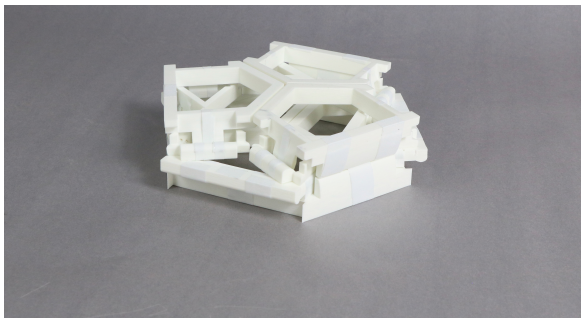

(a) Stowed SORCE panel hexagonal twist.

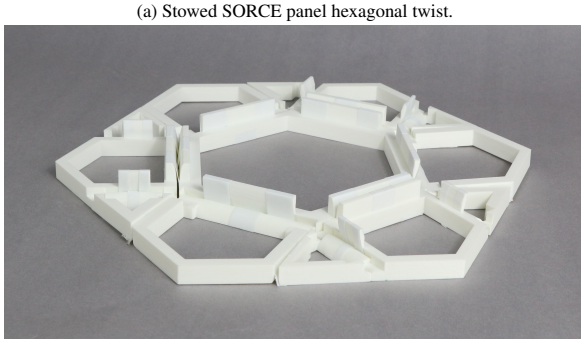

(b) Deployed, open configuration of the SORCE panel hexagonal twist.

**FIGURE 7**: The stowed and deployed states of the SORCE panel hexagonal twist.

## 6 COMPARISON OF TECHNIQUES

### 6.1 Packing Efficiency

Volumes of the different techniques and smallest cuboids were determined using CAD software. In each case, the parameters of the hexagonal pattern were as shown in Table 1. The width of the hinges for the offset panel technique were taken to be the same as the largest width of the SORCE joints as discussed earlier. With these parameters, the packing efficiency of each technique was determined. The values are shown in Table 2.

While these are the packing efficiencies for these given parameters, as the parameters change, these efficiencies will change. With thinner panels, the offset panel hexagonal array

**TABLE 2**: Packing Efficiencies of Three Thickness Accommodation Techniques in the Hexagonal Pattern.

| Accommodation Technique | Packing Efficiency |
|---|---|
| Offset Panel | 0.63 |
| Tapered Panel | 0.27 |
| SORCE Panel | 0.50 |

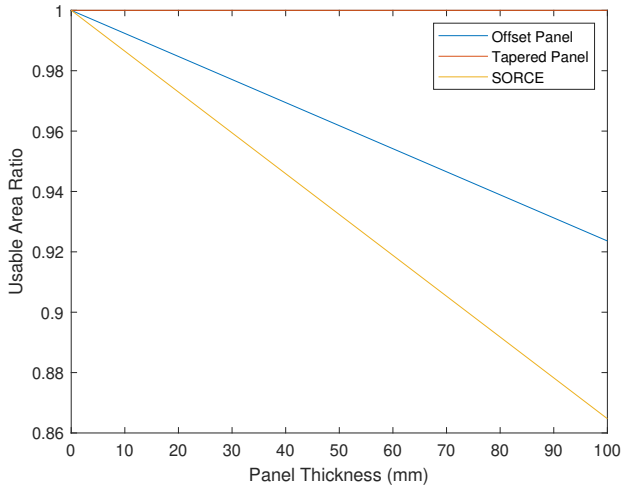


**FIGURE 8**: The usable area ratio as a function of pattern thickness.

can have a packing efficiency around 0.74. With a larger maximum fold angle and panels whose lengths are closer to the thickness, the packing efficiency of teh tapered panel hexagonal array would also increase. An increase could also be achieved in the SORCE joint hexagonal array by using thinner panels.

### 6.2 Usable Deployed Area

Because the SORCE joint widths are dependent on the thickness of the panels, the amount of usable area is dependent on the thickness of the panels. Additionally, the width of the offsets in the offset panel technique can be arbitrarily chosen. To make an equal comparison, the maximum width of the SORCE joints were used as the width of the offsets in the offset panel technique. Because there are no offset hinges in the tapered panel technique, the total area of the hexagon is used and there is no change in usable area for different panel thicknesses. From Fig. 8, the tapered panel has the most usable area, followed by the offset panel, with the SORCE technique having the least amount of usable area. This makes sense because for the offset panel hexagon, there are only 3 offsets occurring on the hexagonal panel and only 3 of the pentagonal panels, while there are SORCE joints on every single panel of the SORCE hexagonal array. As a note, the offsets in the above patterns were assume to extend the total length of each side that they resided on.

### 6.3 End Position of Panels

The offset panel technique provides panels that lie in parallel planes to each other when the pattern is deployed. The offset of the planes is dependent on the thickness of the panels. This offset from the top of the hexagonal pattern to the top of the raised pentagonal and rhombus panels is equal to double the desired total panel thickness ($2t_{panel}$).

The tapered panel technique creates panels where the top of the panels are not parallel. While this is the case, due to the way this technique was determined, there is one plane that all the joints lie on. This provides a method to have a surface internal to the array where all the panels lie on a plane.

The SORCE thickness accommodation technique provides a design where the top of each panel lies in the same parallel plane when the pattern is fully deployed. This allows the designer to avoid having to determine other methods to achieve panels on the same plane.

### 6.4 Effect on Pattern Stability

All three techniques provide inherent hard stops, or places where a panel does not allow another panel to move, stopping the motion at flat, due to panel interference.

The SORCE technique provides at most, half the panel thickness worth of hard stops at the open position. However, the array can still easily roll past these positions. The offset technique provides 2 panel thicknesses of hard stops on 3 sides. The tapered technique provides, at most, half a panel thickness of hardstop on every side. The extent of these hard stops is dependent upon the panel thickness and the selected angle that is desired to have the pattern fold to.

### 6.5 Deployment

**6.5.1 Grounding** In all three techniques, the array could be grounded to the middle hexagonal panel. This would provide a common ground and only the peripheral panels will move around the hexagonal pattern as shown with the deployment in Fig. 1.(b)-(d). All techniques could also be grounded to one of the top folded pentagonal panels. This would allow the pattern to be stowed on the structure, but, when deployed, the array could move away from the center of the structure, which would allow for other potential items to be stowed and deployed from the other end of the structure, such as a feed or receiver. While this is an option for each technique, doing this with the tapered panel technique would decrease the packing efficiency of the array.

**6.5.2 Actuation** Because the position of the joints do not move throughout the deployment motion of the pattern in both the offset panel and tapered panel technique, a rotational actuation system, such as a motor, can be used. This would allow the pattern to be deployed and stowed by rotating an edge or panel of the array. However, this method will not work for the SORCE technique as the joint translates throughout the deployment motion, requiring the motor to translate to accommodate

this motion.

Potential actuation methods that work for all three techniques are using strain energy that is stored (via bending or deflection) in a component. In this case, the SORCE technique could produce a better design technique. This is due to the fact that the joints have a specified curvature. Because the stress in a bending segment is proportional to the curvature, the joints and bending material can be designed to not be overstressed. This is not as easily done with the other techniques.

One other potential actuation method is to use tension-based retraction wires that can be actuated. These could be used to open the pattern, if they were wrapped around the outside of the pattern. They could also be used to close the pattern, if they are attached to the inside of the pattern and then strung through the center of the pattern. In this case, the offsets in all three of the techniques could be used to increase the torque around the joints.

## 7 CONCLUSIONS

This work presents metrics to evaluate thickness accommodation techniques for origami patterns. Three techniques were evaluated using the presented metrics. As with any design application, there are many tradeoffs between each technique and specific design requirements must be used to determine which metrics should be given more weight. For the case of a LIDAR telescope where all the panels ending up on the same plane is very important, the SORCE hexagonal array is the best fit. However, if the requirements of the panels ending in the same plane could be relaxed to the panels only needing to end in parallel planes, then a greater stowability of the pattern could be achieved using the offset panel hexagonal array. Continued work in this area will help to refine metrics and determine the best solutions for each design case.

Future work includes analyzing the trends in packing efficiency as parameters, such as the thickness or maximum fold angle, of the accommodated hexagonal array are changed. Other work could look into better ways to objectively quantify the different types of grounding and actuation options.

## ACKNOWLEDGMENT

This paper is based on work supported by the Air Force Office of Scientific Research grant FA9550-19-1-0290 through Florida International University and the Utah NASA Space Grant Consortium.

## REFERENCES

[1] Moretto, T., and Robinson, R. M., 2008. "Small satellites for space weather research". *Space Weather,* ***6***(5), p. 05007.

[2] Gonzalez-Dorbecker, M., 2015. "Development of tools needed for radiation analysis of a cubesat deployer using oltaris".

[3] Puig-Suari, J., Coelho, R., Williams, S., Aguero, V., Leveque, K., and Klofas, B., 2011. "Recent cubesat launch experiences on us launch vehicles".

[4] Morong, W., Ling, A., and Oi, D., 2012. "Quantum optics for space platforms". *Optics and Photonics News,* ***23***(10), pp. 42–49.

[5] Nayeri, P., Yang, F., and Elsherbeni, A. Z., 2018. *Reflectarray antennas: theory, designs, and applications*. Wiley Online Library.

[6] Huang, J., 2001. "The development of inflatable array antennas". *IEEE Antennas and Propagation Magazine,* ***43***(4), pp. 44–50.

[7] Arya, M., Sauder, J. F., Hodges, R., and Pellegrino, S., 2019. "Large-area deployable reflectarray antenna for cubesats". In AIAA Scitech 2019 Forum, p. 2257.

[8] Sun, X., 2018. "Lidar sensors from space".

[9] Dybal, R. B., 2007. "Satellite antennas". In *Antenna Engineering Handbook*, J. L. Volakis, ed. McGraw-Hill Education.

[10] Yu, M., Yang, W., Yu, Y., Cheng, X., and Jiao, Z., 2020. "A crawling soft robot driven by pneumatic foldable actuators based on miura-ori". In Actuators, Vol. 9, Multidisciplinary Digital Publishing Institute, p. 26.

[11] Sargent, B., Butler, J., Seymour, K., Bailey, D., Jensen, B., Magleby, S., and Howell, L., 2020. "An origami-based medical support system to mitigate flexible shaft buckling". *Journal of Mechanisms and Robotics,* ***12***(4).

[12] Ahmed, A. R., Gauntlett, O. C., and Camci-Unal, G., 2020. "Origami-inspired approaches for biomedical applications". *ACS Omega*.

[13] Yuan, T., Liu, Z., Zhou, Y., and Liu, J., 2020. "Dynamic modeling for foldable origami space membrane structure with contact-impact during deployment". *Multibody System Dynamics,* ***50***(1), pp. 1–24.

[14] Badagavi, P., Pai, V., and Chinta, A., 2017. "Use of origami in space science and various other fields of science". In 2017 2nd IEEE International Conference on Recent Trends in Electronics, Information & Communication Technology (RTEICT), IEEE, pp. 628–632.

[15] Sun, C., Wan, W., and Deng, L., 2019. "Adaptive space debris capture approach based on origami principle". *International Journal of Advanced Robotic Systems,* ***16***(6), p. 1729881419885219.

[16] DeFigueiredo, B. P., Pehrson, N. A., Tolman, K. A., Crampton, E., Magleby, S. P., and Howell, L. L., 2019. "Origami-based design of conceal-and-reveal systems". *Journal of Mechanisms and Robotics,* ***11***(2).

[17] Al-Mansoori, M., Khan, K. A., and Cantwell, W. J., 2020. "Harnessing architected stiffeners to manufacture origami-inspired foldable composite structures". *Composites Sci-*

*ence and Technology,* ***200***, p. 108449.

[18] Wang, L.-C., Song, W.-L., Zhang, Y.-J., Qu, M.-J., Zhao, Z., Chen, M., Yang, Y., Chen, H., and Fang, D., 2020. "Active reconfigurable tristable square-twist origami". *Advanced Functional Materials,* ***30***(13), p. 1909087.

[19] Tolman, K. A., Lang, R. J., Magleby, S. P., and Howell, L. L., 2017. "Split-vertex technique for thickness-accommodation in origami-based mechanisms". In ASME 2017 International Design Engineering Technical Conferences and Computers and Information in Engineering Conference, American Society of Mechanical Engineers Digital Collection.

[20] Lang, R. J., 2017. *Twists, tilings, and tessellations: Mathematical methods for geometric origami*. CRC Press.

[21] Tachi, T., 2011. "Rigid-foldable thick origami". *Origami,* ***5***, pp. 253–264.

[22] Edmondson, B. J., Lang, R. J., Magleby, S. P., and Howell, L. L., 2014. "An offset panel technique for thick rigidily foldable origami". In International Design Engineering Technical Conferences and Computers and Information in Engineering Conference, Vol. 46377, American Society of Mechanical Engineers, p. V05BT08A054.

[23] Lang, R. J., Nelson, T., Magleby, S., and Howell, L., 2017. "Thick rigidly foldable origami mechanisms based on synchronized offset rolling contact elements". *Journal of Mechanisms and Robotics,* ***9***(2).

[24] Lang, R. J., Tolman, K. A., Crampton, E. B., Magleby, S. P., and Howell, L. L., 2018. "A review of thickness-accommodation techniques in origami-inspired engineering". *Applied Mechanics Reviews,* ***70***(1).

[25] Jeong, D., and Lee, K., 2018. "Design and analysis of an origami-based three-finger manipulator". *Robotica,* ***36***(2), pp. 261–274.

[26] Luo, M., Yan, R., Wan, Z., Qin, Y., Santoso, J., Skorina, E. H., and Onal, C. D., 2018. "Orisnake: Design, fabrication, and experimental analysis of a 3-d origami snake robot". *IEEE Robotics and Automation Letters,* ***3***(3), pp. 1993–1999.

[27] Pehrson, N. A., Ames, D. C., Smith, S. P., Magleby, S. P., and Arya, M., 2020. "Self-deployable, self-stiffening, and retractable origami-based arrays for spacecraft". *AIAA Journal,* ***58***(7), pp. 3221–3228.